Dynamical Weights and Enhanced Synchronization in Adaptive Complex Networks

Changsong Zhou and Jürgen Kurths
Institute of Physics, University of Potsdam PF 601553, 14415 Potsdam, Germany

(Received 7 July 2005; revised manuscript received 15 November 2005; published 24 April 2006)

Dynamical organization of connection weights is studied in scale-free networks of chaotic oscillators, where the coupling strength of a node from its neighbors develops adaptively according to the local synchronization property between the node and its neighbors. We find that when complete synchronization is achieved, the coupling strength becomes weighted and correlated with the topology due to a hierarchical transition to synchronization in heterogeneous networks. Importantly, such an adaptive process enhances significantly the synchronizability of the networks, which could have meaningful implications in the manipulation of dynamical networks.

DOI: 10.1103/PhysRevLett.96.164102 PACS numbers: 05.45.Xt, 87.18.Sn, 89.75.−k

Real-world complex networks are interacting dynamical entities with an interplay between dynamical states and interaction patterns. While topological studies have revealed important organization principles in the structures [1], a more complete understanding would require characterizations beyond the topology. There are recently several approaches in this direction. For example, (i) the study of more realistic weighted properties of the connections [2,3]. The analysis of some real networks has shown that the connection weights are often highly heterogeneous and correlated with the degrees [2]. The Barabási-Albert (BA) model [4] has been generalized to take the connection weights into account [3]. (ii) Intensive investigations of synchronization dynamics of oscillatory networks [5–8]. However, most of these works consider networks that do not change with the dynamics, and we call such networks *crystallized networks* (CNs) [9]. (iii) The growing attention on unified studies of the coevolution of dynamical states and network structures [10–14]. Models of *adaptive networks* (ANs) have been proposed, e.g., evolving of nodes due to fitness in interacting species [11], reinforcement of connection strength [12] or rewiring of links [13] due to payoffs among agents playing games; or adaptive changes of coupling strength according to the state distance in globally coupled chaotic maps [14] in a desynchronized regime.

Significant recent interest in synchronization is related to the identification of the network structures that enhance or optimize the global synchronizability. The optimal (unweighted) configurations obtained by optimization algorithms are entangled networks with rather uniform degrees [15], as consistent with graph-theoretical predications [7,16]. However, such topologies do not fit to most realistic network systems. Many complex networks, where synchronization is relevant, are often heterogeneous in topology and are naturally weighted, such as networks of cortical areas [17], networks of cities in the synchronization of epidemic outbreaks [18] and spreading [19]. Thus more interesting is the influence of weighted properties on the synchronizability in degree heterogeneous networks [7,8,16], since suitably weighted connections can enhance significantly the synchronizability without changing the heterogeneity in the topology [7,16]. A question of substantial importance in the light of ANs is whether such weighted properties for enhanced synchronizability can be self-organized.

In this Letter, we study adaptive weight organization and focus on the impacts of heterogeneous topology on the weight structure and on the enhancement of global synchronizability. We introduce a simple, but generic, scheme of weight adaptation according to a local synchronization property, which leads to global synchronization of the whole network. We mainly show that (i) the network becomes weighted and the weights are negatively correlated with the degrees, and (ii) importantly, the adaptation enhances significantly the synchronizability compared to unweighted CNs.

We consider N coupled identical chaotic oscillators

$$\dot{\mathbf{x}}_i = \mathbf{F}(\mathbf{x}_i) + \sum_{j=1}^{N} G_{ij}[\mathbf{H}(\mathbf{x}_j) - \mathbf{H}(\mathbf{x}_i)], \qquad (1)$$

where $\mathbf{F}(\mathbf{x})$ is the dynamics of individual oscillators and $\mathbf{H}(\mathbf{x})$ is the linear output function. $G = (G_{ij})$ is the weighted coupling matrix, $G_{ij} = A_{ij}W_{ij}$, where A_{ij} is the binary adjacency matrix and $W_{ij} > 0$ is the coupling strength from node j to node i if they are connected. In unweighted networks, $W_{ij} = 1$ is uniform for all links. In previous studies of CNs [5–8], $G_{ij} = \sigma G^0_{ij}$, where G^0_{ij} is fixed and σ controls the overall strength of the connections.

Here we study ANs where the coupling strengths W_{ij} is controlled by the *local* synchronization properties of the nodes. To achieve a global synchronization of the network, it is natural to assume that each node tries to synchronize to its neighbors by increasing the coupling strength from them. We suppose that the strength to a node i from all its k_i neighbors increases uniformly among the k_i connections, in order to suppress its difference Δ_i from the mean activity of its neighbors, namely,

$$G_{ij}(t) = A_{ij}V_i(t), \qquad \dot{V}_i = \gamma\Delta_i/(1 + \Delta_i), \qquad (2)$$

where $\Delta_i = |\mathbf{H}(\mathbf{x}_i) - (1/k_i)\sum_j A_{ij}\mathbf{H}(\mathbf{x}_j)|$, and $\gamma > 0$ is the adaptation parameter. We assume that the initial coupling strength is small, a random value. Such an adaptation scheme is probably the simplest, but it is based on a generic dynamical feedback principle, e.g., adopted in controlling a chaotic oscillator to stable dynamics [20]. With this adaptation scheme, the input weight ($W_{ij} = V_i$) and the output weight ($W_{ji} = V_j$) of a node i are in general asymmetrical.

We consider scale-free networks (SFNs) (matrix A) generated with the BA model [4]. Starting with M fully connected nodes (with labels $i = 1, 2, \ldots, M$), at each time step $T = 1, 2, \ldots, (N - M)$ a new node (with label $i = M + T$) is added and connected to M existing nodes in the network. Thus, nodes with smaller i in general have larger degrees k_i. The resulting SFNs have a degree distribution $P(k) \sim k^{-\Gamma}$, with $\Gamma = 3$ and the minimal degree $k_{\min} = M$.

First we briefly review the stability of CNs [6],

$$\dot{\mathbf{x}}_i = \mathbf{F}(\mathbf{x}_i) + \sigma \sum_{j=1}^{N} G_{ij}^0 [\mathbf{H}(\mathbf{x}_j) - \mathbf{H}(\mathbf{x}_i)]. \tag{3}$$

The variational equations of Eq. (3) with respect to the complete synchronization state ($\mathbf{x}_i = \mathbf{s}, \forall\ i$) is diagonalized into N eigenmodes of the form $\dot{\xi}_i = [D\mathbf{F}(\mathbf{s}) - \sigma\lambda_i \mathbf{H}(\mathbf{s})]\xi_i$, which are only different by the eigenvalue λ_i of the Laplacian matrix $L = (L_{ij})$ [6], where $L_{ij} = -G_{ij}^0 + \delta_{ij}\sum_j^N G_{ij}^0$. We treat the case that the spectra of eigenvalues are real and can be ordered as $0 = \lambda_1 \leq \lambda_2 \cdots \leq \lambda_N$, with $\lambda_1 = 0$ associated with the invariance of the state $\mathbf{s}$. The largest Lyapunov exponent (LLE) $\Lambda(\epsilon)$ of the modes as a function of $\epsilon = \sigma\lambda_i$, known as the master stability function (MSF) [6], is negative in an interval $\epsilon_1 < \epsilon < \epsilon_2$ for general output function $\mathbf{H}(\mathbf{x})$. The state $\mathbf{s}$ is stable when all the nontrivial eigenmodes $i \geq 2$ have negative LLE, namely,

$$\epsilon_1 < \sigma\lambda_2 \leq \cdots \leq \sigma\lambda_N < \epsilon_2. \tag{4}$$

For the special case $\epsilon_2 = \infty$, the state $\mathbf{s}$ is stable for $\sigma > \epsilon_1/\lambda_2$. In the general case of finite ϵ_2, $\mathbf{s}$ is stable for $\epsilon_1/\lambda_2 < \sigma < \epsilon_2/\lambda_N$ if the eigenratio $R \equiv \lambda_N/\lambda_2 < \epsilon_2/\epsilon_1 \equiv R_\epsilon$. However, if $R > R_\epsilon$, Eq. (4) can never be fulfilled, and it is impossible to synchronize the networks. It is R that is minimized using optimization algorithms in Ref. [15].

In ANs, the weights W_{ij} and suitable σ values are obtained adaptively. Synchronization can be achieved for many large networks which are otherwise not synchronizable when unweighted. This general behavior is illustrated by the chaotic Rössler oscillator: $\mathbf{x} = (x, y, z)$ and $\mathbf{F}(\mathbf{x}) = (-0.97x - z, 0.97x + 0.15y, x(z - 8.5) + 0.4)$ and a chaotic foodweb model [21]: $\mathbf{F}(\mathbf{x}) = (x - 0.2g(x, y), -0.7y + 0.2g(x, y) - xz, -10x(z - 0.006) + xz)$, where $g(x, y) = xy/(1 + 0.05x)$.

We consider both cases $\epsilon_2 = \infty$ and $\epsilon_2 < \infty$. The case $\epsilon_2 = \infty$ can be realized with $\mathbf{H}(\mathbf{x}) = \mathbf{x} = (x, y, z)$ since $\Lambda(\epsilon) = \Lambda_F - \epsilon$, where $\Lambda_F > 0$ is the LLE of the isolated oscillator $\dot{\mathbf{x}} = \mathbf{F}(\mathbf{x})$. Then, the ANs are synchronizable for any nonvanishing $\gamma > 0$, with faster converging rates at larger γ values. The transition to synchronization is shown in Fig. 1(a). Starting from random initial conditions on the chaotic attractors, the local synchronization difference $\Delta_i \gg 1$, and the input weights of each node increase uniformly in the whole network, i.e., $W_{ij} = V_i(t) \approx \gamma t$ [Fig. 1(a), inset]. After a short period, the weights V_i of different nodes develop at different rates and converge to different values $\tilde{V}_i$: the input strength is smaller on average for nodes with larger degrees k_i (smaller i) [Fig. 1(b)].

The dependence of the input strength of a node on its degree becomes more evident when we plot the average value $V(k) = (1/N_k)\sum_{k_i=k}\tilde{V}_i$ for all the N_k nodes with degree k, in a larger network of $N = 1000$ nodes [Fig. 2(a)]. The results display a power law

$$V(k) \sim k^{-\theta}, \tag{5}$$

with an exponent $\theta = 0.48 \pm 0.01$ for both oscillator models. Importantly, this scaling is also robust to variation of network parameters, such as the minimal degree M [Fig. 2(b)] and the system size N [Fig. 2(c)]. It holds also for various orders of magnitudes of the adaptation parameter γ [Fig. 2(d)]. We have also examined another network model which generates SFNs with a varying exponent Γ due to aging affects of the nodes [22], and the scaling in Eq. (5) with the same exponent θ holds for a broad range of Γ values, and for exponential degree distributions, too.

Equation (5) results from a hierarchical transition to synchronization in the network due to heterogeneous degrees. Since $W_{ij}(t) = V_i(t)$, Eq. (1) can be rewritten as $\dot{\mathbf{x}}_i = \mathbf{F}(\mathbf{x}_i) + S_i(t)[\mathbf{H}(\bar{\mathbf{x}}_i) - \mathbf{H}(\mathbf{x}_i)]$, where $\bar{\mathbf{x}}_i = (1/k_i) \times \sum_{j=1}^N A_{ij}\mathbf{x}_j$ is the local mean field of all the neighbors connected to the oscillator i. Here $S_i(t) = k_i V_i(t)$, the total input weights of node i, represents the *intensity* of the node. In random networks the local mean field $\bar{\mathbf{x}}_i$ of nodes with $k_i \gg 1$ can be approximated by the global mean field of the network, $\bar{\mathbf{x}}_i \approx \mathbf{X}$, and we get

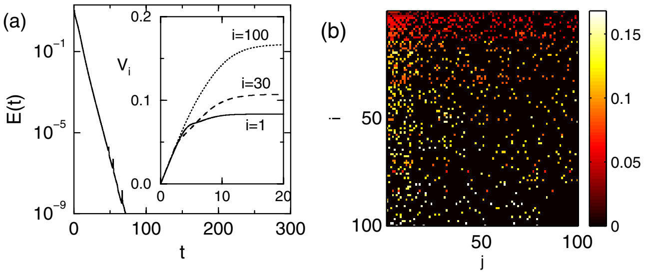

FIG. 1 (color online). (a) Transition to synchronization in an AN of Rössler oscillators, indicated by the synchronization error averaged on the nodes: $E(t) = \langle|\mathbf{x}_i - \langle\mathbf{x}_i\rangle|\rangle$. Inset: the input strength $V_i(t)$ vs time for three nodes. (b) The weighted coupling matrix $\tilde{G}$ crystallized after the adaptation (for the foodweb model). Here $M = 5$, $N = 100$, and $\gamma = 0.02$.

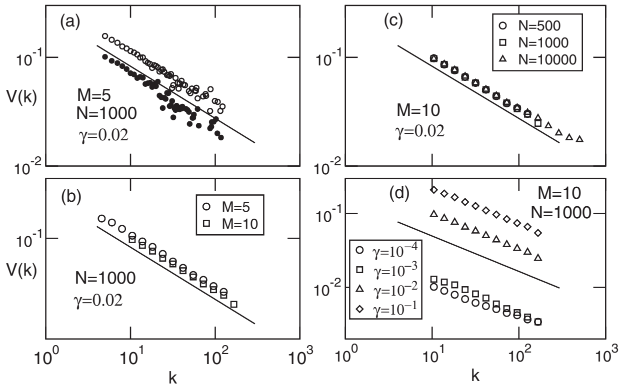

FIG. 2. The average input weight $V(k)$ of nodes with degree k as a function of k for the Rössler oscillators (○) and the foodweb model (●) (a) and its dependence on various parameters: M (b), N (c), and γ (d). Results in (b), (c), (d) are averaged over 10 realizations of the networks with random initial conditions. For clarity, only the results for the Rössler oscillators are shown in (b), (c), (d) and are logarithmically binned. The solid lines in (a), (b), (c), (d) have a slope -0.48.

$$\dot{\mathbf{x}}_i \approx \mathbf{F}(\mathbf{x}_i) + S_i(t)[\mathbf{H}(\mathbf{X}) - \mathbf{H}(\mathbf{x}_i)]. \tag{6}$$

Under this approximation, the oscillators are forced by a common mean field signal $\mathbf{H}(\mathbf{X})$ with the forcing strength $S_i(t)$. When the adaptation starts, $V_i(t) \approx \gamma t$ [Fig. 1(a), inset], so that $S_i(t) \approx \gamma k_i t$. As a result, nodes with larger degrees k are coupled more strongly to the forcing signal $\mathbf{H}(\mathbf{X})$. When $\mathbf{H}(\mathbf{x}) = \mathbf{x}$, the LLE of Eq. (6) $\Lambda(S_i) = \Lambda_F - S_i$, so that nodes with larger degrees k will synchronize faster to the mean activity of its neighbors. Hence Δ in Eq. (2) decreases with k. Because of this hierarchical transition to synchronization, nodes with larger degree k have smaller increasing rates of the weight $V(k)$ in Eq. (2), which results in the relation of Eq. (5). This mechanism does not depend on particular oscillators and degree distributions.

Now we analyze the typical case of finite ϵ_2. In the Rössler oscillators, this happens, e.g., with $\mathbf{H}(\mathbf{x}) = (x, 0, 0)$. In the foodweb model, the ecologically realistic coupling (immigration) [21] denoted by $\mathbf{H}(\mathbf{x}) = (0, y, z)$ results in a very similar MSF [Fig. 3(a)]. We find that an almost linear decrease of $\Lambda(\epsilon)$ in the small ϵ region is a common property of MSF for general $\mathbf{H}(\mathbf{x})$ and $\mathbf{F}(\mathbf{x})$. With small enough γ, the ANs are operating in this region in the beginning of the adaptation and the hierarchical transition to synchronization occurs basing on Eq. (6). In our simulations with networks as large as $N = 10^4$ (BA model, $M = 5$), synchronization can always be achieved by the adaptation of Eq. (2) if it is not too fast, i.e., $\gamma \leq \gamma_c$, where γ_c depends slightly on N and the oscillator models. The resulting weighted networks display the same power-law behavior in Eq. (5), but with slightly different exponents: $\theta = 0.54 \pm 0.01$ (Rössler oscillator) and $\theta = 0.36 \pm 0.01$ (foodweb). However, in unweighted CNs, i.e., $G_{ij} = \sigma A_{ij}$, synchronization becomes impossible for $N \gtrsim 1000$ (Rössler) and $N \gtrsim 500$ (foodweb).

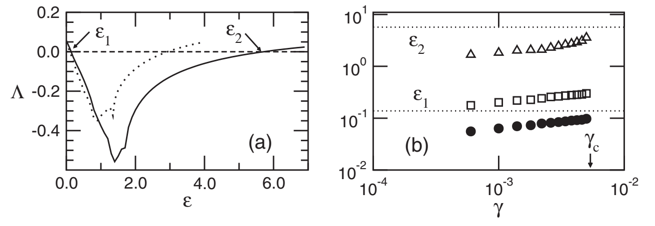

FIG. 3. (a) MSF Λ vs ϵ. Solid line: Rössler oscillator with $\mathbf{H}(\mathbf{x}) = (x, 0, 0)$; dotted line: foodweb model with $\mathbf{H}(\mathbf{x}) = (0, y, z)$. (b) σ (●), $\sigma\lambda_2$ (□), and $\sigma\lambda_N$ (△) vs γ in adaptive networks of Rössler oscillators with $M = 5$, $N = 1000$, and $\mathbf{H}(\mathbf{x}) = (x, 0, 0)$. Dotted lines: the two thresholds ϵ_1 and ϵ_2.

We stress that the weighted structures [Eq. (5)] are almost crystallized (saturated) after a short period of adaptation [Fig. 1(a), inset]; afterwards the transition to synchronization is similar to CNs. The strongly enhanced synchronizability by the adaptation thus can be understood by the stability of the CNs [Eq. (3)], by comparing the weighted networks ($G^0 = \tilde{G}$) with the unweighted counterparts ($G^0 = A$). Here $\tilde{G}$ obtained by the adaptation has been normalized so that $\langle \tilde{G}_{ij} \rangle_{A_{ij}=1} = 1$ as in the matrix A.

We have calculated σ and the spectra of the weighted networks obtained at various γ values, as shown in Fig. 3(b) for the Rössler oscillators. When γ is very small, the weight adaptation is adiabatic and $\sigma\lambda_2$ is slightly above the lower threshold ϵ_1. Both $\sigma\lambda_2$ and $\sigma\lambda_N$ increases as γ increases till the critical value γ_c. For $\gamma > \gamma_c$, the adaptation process generates in the beginning a similar weighted structure as for $\gamma < \gamma_c$, but in a moment, $\sigma\lambda_N > \epsilon_2$ the synchronization errors grow again, leading to desynchronization of the whole network.

The synchronizability can be assessed further by the eigenratio $R = \lambda_N/\lambda_2$ [6,7]. If the adaptation leads to almost saturated weighted networks with $R < \epsilon_2/\epsilon_1$ in the early stage, it will achieve global synchronization. R is statistically independent of small γ. We calculate R for the weighted networks after the adaptation and compare to R of unweighted networks, as a function of N [Fig. 4(a)]. As

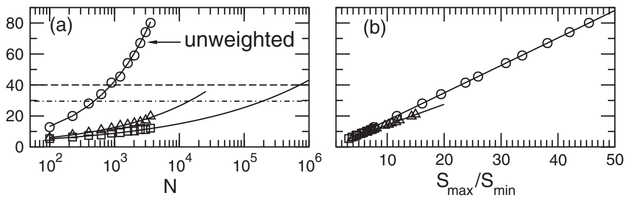

FIG. 4. The eigenratio R as a function of N (a) and $S_{\max}/S_{\min}$ (b), averaged over 20 realizations of the networks. The solid lines are power-law (a) and linear (b) fitting. The weighted networks are obtained by the adaptive process with the conditions: $M = 5$, $\gamma = 0.002$ with $\mathbf{H}(\mathbf{x}) = (x, 0, 0)$ for the Rössler oscillators (□), and $\mathbf{H}(\mathbf{x}) = (0, y, z)$ for the foodweb model (△). The networks are synchronizable if $R < R_\epsilon$ in (a): Rössler oscillators, $R_\epsilon = 40$ (dashed line), foodweb model, $R_\epsilon = 29$ (dashed-dotted line).

consistent with our recent graph-spectral analysis [16], R increases linearly with $S_{\max}/S_{\min}$ [Fig. 4(b)], for both networks. $S_{\max}$ and $S_{\min}$ are the maximum and minimum of the intensities S_i, and $S_{\max}/S_{\min} = k_{\max}/k_{\min} \sim N^{1/2}$ in the unweighted BA model. In ANs, we have $S_{\max}/S_{\min} \sim N^{\beta/2}$ with $\beta = 1 - \theta$, since $S_i = k_i V_i \sim k^{\beta}$ according to Eqs. (2) and (5). Thus $R \sim N^{\alpha}$, with $\alpha = \frac{1}{2}$ and $\alpha = \frac{\beta}{2}$ for the unweighted and weighted networks, respectively [Fig. 4(a), solid lines]. The adaptation process enhances synchronization since $S_{\max}/S_{\min}$ is significantly reduced during the transition to synchronization. While the unweighted CNs are already impossible to synchronize for $N > N_1 \approx 10^3$ (Rössler) and $N_1 \approx 500$ (foodweb), in sharp contrast, the ANs are synchronizable till $N_2 \approx 8 \times 10^5$ (Rössler) and $N_2 \approx 1.5 \times 10^4$ (foodweb). The degree of enhancement can be expressed as $N_2/N_1 \approx R_{\epsilon}^{1/\beta}$ for SFNs [$P(k) \sim k^{-\Gamma}$] regardless of Γ. Since $\beta < 1$ ($\sim$0.5), a significantly enhanced synchronizability is expected for general $\mathbf{F}(\mathbf{x})$ and $\mathbf{H}(\mathbf{x})$ with $R_{\epsilon} = \epsilon_2/\epsilon_1 \gg 1$.

It is interesting to compare the weighted properties resulting from the adaptive synchronization to those observed in real networks, including scientific collaboration networks [2], metabolic networks [23], or airport networks [2,23]. There it has been shown that the intensity S_i of the nodes, defined as $S_i = \sum_{j=1}^{N} A_{ij} W_{ij}$ in general networks, provides a significant measure integrating the information of connectivity and weights. The average value $S(k)$ over nodes of degree k increases as $S(k) \sim k^{\beta}$, with the exponent β varying as a function of the specific network. In our adaptive networks, we also have $S(k) \sim k^{\beta}$ with $\beta \sim 0.5$. The case $\beta < 1$ corresponds to a saturation in the intensity of the nodes with large degrees and is also observed in realistic neuronal networks [24] where synchronization plays an important role in the information processing. Importantly, we have shown that the ability of the networks to achieve synchronization is significantly enhanced, since the heterogeneity of the intensities is reduced adaptively. The detailed mechanisms underlying the weight and topological structures of specific real networks are often different, e.g., synaptic plasticity in neuronal networks [25], degree-dependent traffic load in airport networks [26], or overload-driven evolution in electric grids [10]. A general principle beyond these mechanisms is an enhanced or optimized functionality of the particular network systems due to the interplay and the coevolution of the network structure and dynamics. Here we consider the idealized case of global synchronization. More realistic systems such as brain displays a scale-free organization of the synchronization patterns [27] arising from the underlying hierarchical complex neural networks [17]. Understanding the self-organization of such large-scale complex structures and dynamics is still a big challenge.

This work was supported by Promotionskolleg, EU-Network BioSim, Contract No. LSHB-CT-2004-005137, and the DFG Forschergruppe Conflicting Rules.

[1] R. Albert and A.-L. Barabási, Rev. Mod. Phys. **74**, 47 (2002).

[2] A. Barrat *et al.*, Proc. Natl. Acad. Sci. U.S.A. **101**, 3747 (2004).

[3] S. H. Yook, H. Jeong, A.-L. Barabási, and Y. Tu, Phys. Rev. Lett. **86**, 5835 (2001); A. Barrat, M. Barthélemy, and A. Vespignani, *ibid.* **92**, 228701 (2004).

[4] A.-L. Barabási and R. Albert, Science **286**, 509 (1999).

[5] J. Jost and M. P. Joy, Phys. Rev. E **65**, 016201 (2002); M. Timme, F. Wolf, and T. Geisel, Phys. Rev. Lett. **89**, 258701 (2002); T. Nishikawa *et al.*, *ibid.* **91**, 014101 (2003); V. N. Belykh, I. V. Belykh, and M. Hasler, Physica (Amsterdam) **195D**, 159 (2004).

[6] M. Barahona and L. M. Pecora, Phys. Rev. Lett. **89**, 054101 (2002).

[7] A. E. Motter, C. S. Zhou, and J. Kurths, Europhys. Lett. **69**, 334 (2005); Phys. Rev. E **71**, 016116 (2005).

[8] M. Chavez *et al.*, Phys. Rev. Lett. **94**, 218701 (2005).

[9] Random change of network topology *independent of oscillatory dynamics* has been considered in I. V. Belykh, V. N. Belykh, and M. Hasler, Physica (Amsterdam) **195D**, 188 (2004).

[10] A. Scirè, I. Tuval, and V. M. Eguíluz, Europhys. Lett. **71**, 318 (2005).

[11] S. Jain and S. Krishna, Proc. Natl. Acad. Sci. U.S.A. **98**, 543 (2001).

[12] B. Skyrms and R. Pemantle, Proc. Natl. Acad. Sci. U.S.A. **97**, 9340 (2000).

[13] M. G. Zimmermann, V. M. Eguíluz, and M. S. Miguel, Phys. Rev. E **69**, 065102 (2004).

[14] J. Ito and K. Kaneko, Phys. Rev. Lett. **88**, 028701 (2002); Phys. Rev. E **67**, 046226 (2003).

[15] L. Donetti, P. I. Hurtado, and M. A. Muñoz, Phys. Rev. Lett. **95**, 188701 (2005).

[16] C. S. Zhou, A. E. Motter, and J. Kurths, Phys. Rev. Lett. **96**, 034101 (2006).

[17] J. W. Scannell *et al.*, Cereb. Cortex **9**, 277 (1999).

[18] B. T. Grenfell *et al.*, Nature (London) **414**, 716 (2001).

[19] L. Hufnagel, D. Brockmann, and T. Geisel, Proc. Natl. Acad. Sci. U.S.A. **101**, 15 124 (2004).

[20] D. Huang, Phys. Rev. Lett. **93**, 214101 (2004).

[21] B. Blasius, A. Huppert, and L. Stone, Nature (London) **399**, 354 (1999).

[22] S. N. Dorogovtsev and J. F. F. Mendes, Phys. Rev. E **62**, 1842 (2000).

[23] P. J. Macdonald *et al.*, cond-mat/0405688.

[24] G. Zamora, C. Zhou, and J. Kurths (unpublished).

[25] G. Bi and M. Poo, J. Neurosci. **18**, 10 464 (1998).

[26] K.-I. Goh, B. Kahng, and D. Kim, Phys. Rev. E **72**, 017103 (2005).

[27] V. M. Equíluz *et al.*, Phys. Rev. Lett. **94**, 018102 (2005).